3D parameter to quantify the anisotropy measurement of periodic structures on rough surfaces

Gildas Guillemot, Maxence Bigerelle, Zahra Khawaja

3D Parameter to Quantify the Anisotropy Measurement of Periodic Structures on Rough Surfaces

G. Guillemot,[1] M. Bigerelle,[2] and Z. Khawaja[3]

[1]CEMEF, Centre de Mise en Forme des Matériaux, MINES ParisTech, Rue Claude Daunesse, Sophia Antipolis, France
[2]Laboratoire Thermique, Energétique, Mise en forme, Production LAMIH/TEMPO UMR 8201, Université de Valenciennes et du Hainaut Cambrésis, Le Mont Houy, Valenciennes, France
[3]Laboratoire Roberval, UMR 6253, UTC/CNRS, Centre de recherche de Royallieu, Compiègne, France

Summary: In this paper, a new 3D roughness parameter, S_{reg}, is proposed to quantify the regularity of a surface, independent of the amplitude and the scanning length units of the surface. The efficiency of this parameter is tested on noisy periodical surfaces with degrees of anisotropy. This parameter lies between zero (perfect noise) and 100% (a perfect periodic surface). This parameter enables the identification of the anisotropy directions of regularity for a given surface. For a periodical surface, the greater the noise, the lower the anisotropy. A direction function is proposed to analyse the direction of regularity of a rough surface, which then permits characterization of the directional regularity of the topography. The regularity parameter can be used for several purposes: to identify the direction of periodical structures formed by laser-pulsed radiations on the surface of solid workpieces; to examine the reproducibility of surface machining methods such as finishing process; and to identify the surface regularity produced by abrasive machining, such as precision surface grain, abrasive slotting, and lapping. SCANNING 36: 127–133, 2014. © 2013 Wiley Periodicals, Inc.

Key words: surface roughness, statistical analysis, surface regularity, 3D roughness parameter

Introduction

Surface roughness refers to the evolution of the surface compared with the mean of the surface. The standard DIN4760 defines the orders of deviation (DIN4760, '82). Benardos and Vasniakos (2003) describe these orders. They indicate that:

- First and second orders of deviation relate, respectively, to the form (i.e., flatness, circularity, etc.) and to waviness. These deviations are due to machine tool errors, deformation of the workpiece, erroneous setups, clamping, vibration, and workpiece material in homogeneity.
- Third and fourth orders of deviation refer to periodic grooves, cracks, and erosions, which are connected to the shape and condition of the cutting edges, to chip formation, and to kinematics processes.
- Fifth and sixth orders of deviation refer to the material structure of the workpiece, which is connected to physical–chemical mechanisms acting on a grain and to lattice scale (slip, diffusion, oxidation, residual stress, etc.).

Many parameters associated with machining processes and/or workpiece properties influence surface roughness. Figure 1 represents an ordered nonexhaustive diagram of these parameters. Consequently, studies of the surface topography of manufactured elements are developed with two principal objectives of analysis: the effect of machining parameters and the adverse consequences in the workpiece properties (Venkateh et al., '99a,b). Different roughness parameters have been proposed to qualify a machined surface. The more common parameters are: the arithmetical mean height of the surface (S_a), the root mean square height of the surface (S_q), and the maximum height of the surface (S_z). These parameters do not disclose the complexity of the surface (Bhushan, '99). Nevertheless, this paper proposes to quantify the organization of surfaces
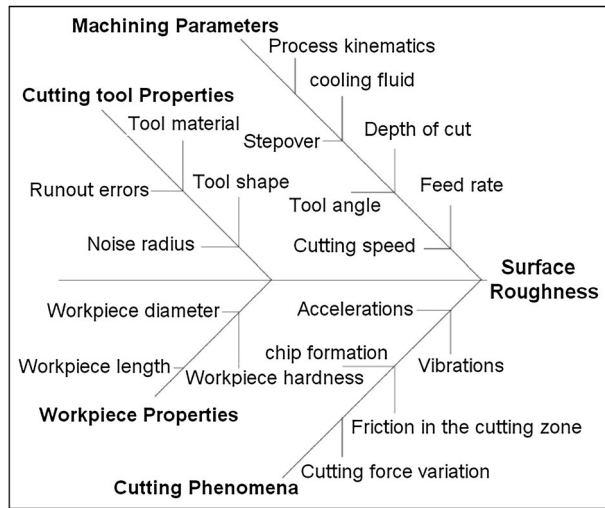
Fig 1. diagram representing paramters that influence surface roughness (Benardos and Vasniakos, 2003).

through the integration of a new scale invariant roughness parameter. This parameter is called the "regularity parameter," and it is used in order to identify the influence of various processes on the topography of a machined surface.

The Regularity Parameter

Mathematical Definition

Fourier analysis is a well-known signal processing method used in surface topography (Whitehouse, 2011), widely used in solving engineering problems. However, in some applications such as surface roughness characterization, this method is not necessarily the most appropriate one, particularly to treat multi-scale aspects of the morphology (Dubuc *et al.*, '89). Indeed, the relevance of parameters calculated from Fourier analysis on "industrial" 2D surfaces is weak (Dong and Stout, '95). If the surface cannot clearly show periodic structures, no precise analysis can be developed with Fourier analysis (Chien *et al.*, 2011). Moreover the calculation of a single scalar parameter corresponding to the whole Fourier transformation signal leads to a loss of information (Mallat, '89). Ultimately, Fourier analysis does not enable the definition of the "regularity" of a surface (Weiting *et al.*, 2009). This "regularity" should correspond to the level of the reproducibility of the same "sub-signal" or "sub-information" on the whole signal (Novák *et al.*, 2009). Therefore, to study the regularity of a surface, a regularity parameter is proposed. It is supposed that the parameter has an upper limit value of 100% for perfect 2D periodic surfaces and a lower limit value of 0% for uncorrelated 2D random surfaces

("white noise"). To calculate this parameter the following steps are applied:

First, a normalized autocorrelation function (ACF) is defined for any integers X and Y, such that: Other papers do not use Boldface in equations

$$\mathbf{ACF}(X, Y) = \frac{1}{S_q^2 (n-X)(m-Y)} \sum_{i=1}^{n-X} \sum_{j=1}^{m-Y} z_{i,j} z_{i+X, j+Y} \tag{1}$$

where $Z_{i,j}$ is the value of the signal for the point (i, j) (i.e., *height of the surface*) with $1 \leq i \leq n$ and $1 \leq j \leq m$. S_q is the well-known standard deviation of the amplitude (root mean square parameter) of the surface.

In order to express this function in polar coordinates, Cartesian coordinates (X, Y) are changed to polar coordinates (R, θ). The ACF function will be considered as expressed in polar coordinates (i.e., $\mathbf{ACF}(R, \theta)$) until the end of this paper.

Secondly, an autocorrelation length $l(\theta, \lambda)$ for a fixed threshold value of the autocorrelation function $\mathbf{ACF}(R, \theta)$ is defined in terms of polar coordinates (R, θ). This value, l, depends on the threshold value, λ, and corresponds to the last value R, such that $\mathbf{ACF}(R, \theta) \geq \lambda$. λ is also called the inverse lag length and is taken as equal to 0 in this paper.

Then, a correlation integral $j(\theta, \lambda)$ is introduced:

$$j(\theta, \lambda) = \int_0^{l(\theta, \lambda)} ACF(R, \theta) \; \mathrm{d}R \tag{2}$$

Thirdly, the series $i_k(\theta, \lambda)$ of integrals is defined:

$$i_k(\theta, \lambda) = \int_{k/(\theta, \lambda)}^{(k+1)l(\theta, \lambda)} ACF(R, \theta) \; \mathrm{d}R \tag{3}$$

with $1 \leq k \leq k_{\max}$. $k_{\max}$ corresponding to the maximum value of index k in any θ direction. Thus, $(k_{\max} + 1) l(\theta, \lambda)$ is lower than the minimum length of the signal in any direction. This latter value corresponds to the minimum value between n and m. The sequence of i_k values represents a kind of successive harmonics of the regularity of the surface.

Finally, the regularity vector, $S_{\mathrm{reg}}(\theta, \lambda)$, is defined for any (θ, λ) value as:

$$S_{\mathrm{reg}}(\theta, \lambda) = 100 \frac{\sum_{k=1}^{k_{\max}} i_k(\theta, \lambda)}{k_{\max} j(\theta, \lambda)} \tag{4}$$

This parameter lies between 0 (uncorrelated random surfaces) and 100 (perfect periodic surfaces without noise). Its most important property is to be mathematically independent of the amplitude parameter. The

scalar mean regularity parameter, $S_{\text{reg}}(\lambda)$, is defined as the mean of the regularity vector, $S_{\text{reg}}(\theta, \lambda)$ elements:

$$S_{\text{reg}}(\lambda) = \frac{\sum_{p=1}^{N_\theta} S_{\text{reg}}(\theta_p, \lambda)}{N_\theta} \tag{5}$$

where N_θ corresponds to the number of regularly spaced θ_p values that have been studied. Usually, this value lies between 100 and 200, in order to cover a sufficiently large set of directions into the plane.

Simulated Examples

To test the relevance of the defined regularity parameter, S_{reg}, in the measurement of the order of surfaces, a large number of square surface shapes have been simulated. Each surface contains $1,000 \times 1,000$ points, uniformly distributed on a square. These shapes are gathered in four sets:

- The first set of surface shapes is a distribution of Gaussian noise, having a null mean value and standard deviation of 1. These surfaces are named "Gaussian noisy surfaces" with symbol W_N.
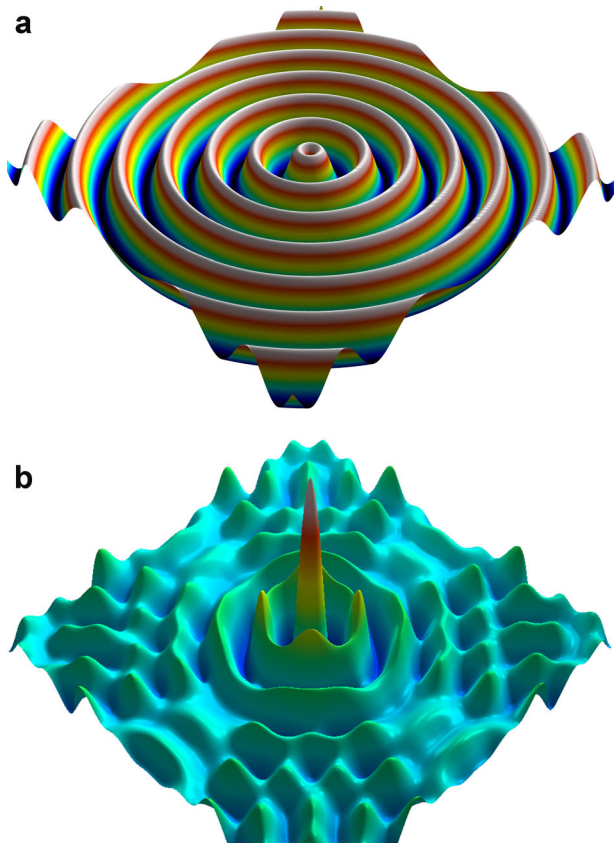- The second set has the form of concentric open cylinders, identified as polar surfaces (see Fig. 2).

Fig 2. (a) Isotropic polar surface and (b) its associated autocorrelation function.

This set is obtained by sweeping a sinusoidal signal around the amplitude axis (Z-axis).

- The third set has the form of homogeneously distributed bumps, identified as isotropic sine surfaces (see Fig. 3a). This set is obtained by multiplying together two trigonometric functions. In these surfaces, the perfect sine form is clearly identified in the X and Y directions. Then a stationary uncorrelated Gaussian noise W_N is added to these surfaces.

$$Z(x,y) = \sin(2\pi x) \times \cos\left(2\pi y + \frac{\pi}{2}\right) + \sigma W_N \tag{6}$$

where σ represents the noise level, and W_N is a distribution of Gaussian noise having a null mean value and a standard deviation equal to 1.

For a given set, different levels of noise are attributed. Figure 3b and c shows, respectively, the effect of the added Gaussian noise on sine surfaces. At zero noise level, the surface shape is distinctly outlined (see Fig. 3a). As noise level increases, the amplitude of the surface increases, and its shape becomes more and more deformed (see Fig. 3b at 0.1 noise level). At a 1 noise level, the shape of the surface is scarcely recognizable (see Fig. 3c). The shape will continue to be deformed until it reaches the form of a Gaussian noise. At a level of 1.8, the sine shape surfaces have pure Gaussian noise forms and cannot be distinguished.

- The fourth set is composed of anisotropic sine surfaces that allow testing of the directions of anisotropy. This set is named "anisotropic sine surfaces" and is obtained by multiplying together two trigonometric functions and incorporating a factor α, as represented in Equation 7. For $\alpha = 1$, the obtained surface has an isotropic sine shape (see Fig. 3a).

$$Z(x,y) = \sin(2\pi x) \times \cos\left(2\frac{1.5\pi y}{1.5^\alpha} + \frac{\pi}{2}\right) + \sigma W_N \tag{7}$$

The number of bumps on the sine surfaces decreases when the anisotropy factor increases, because the wavelength of these surfaces in the Y direction increases when the value of the factor increases. For example, a sine surface whose anisotropy factor is equal to 2 (represented in Fig. 4a) has a shorter wavelength than a surface whose anisotropy factor is equal to 4 (represented in Fig. 4b). For high value of anisotropy factor, the 3D sinus shape converges to a 2D sinus and becomes perfectly orthotropic (Fig. 4c). The value of the factor α varies between 1 (isotropic sine surface) and 16 (high anisotropic sine surface).

Results and Discussion

In order to evaluate the direction of the anisotropy on a surface, polar coordinates are used. For each surface, 181 regularity parameters are calculated by varying the
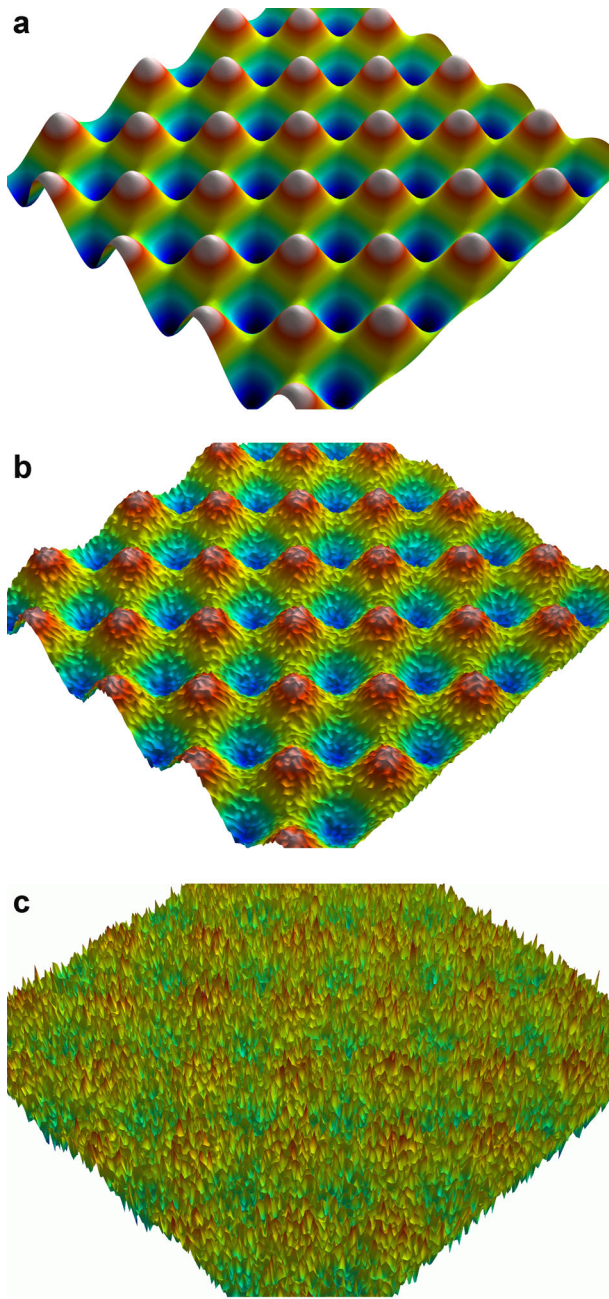
Fig 3.   Isotropic sine shape: (a) noise $= 0$, (b) noise $= 0.1$, and (c) noise $= 1$.

Fig 4.   A sine surfaces with different anisotropy factors: (a) $\alpha = 2$, (b) $\alpha = 4$, and (c) $\alpha = 16$.

angle θ between $0°$ and $180°$. These calculated values are used to draw the curve that represents the regularity values $(X_r(\theta), Y_r(\theta))$, where $X_r(\theta)$ is the projection of the regularity vector on the X axis, given by:

$$X_r(\theta) = S_{\mathrm{reg}}(\theta) \times \cos(\theta) \qquad (8)$$

And $Y_r(\theta)$ is the projection of the regularity vector on the Y axis, given by:

$$Y_r(\theta) = S_{\mathrm{reg}}(\theta) \times \sin(\theta) \qquad (9)$$

Figure 5 represents the anisotropy direction curves of the surfaced shaped by Gaussian noise. The curves have
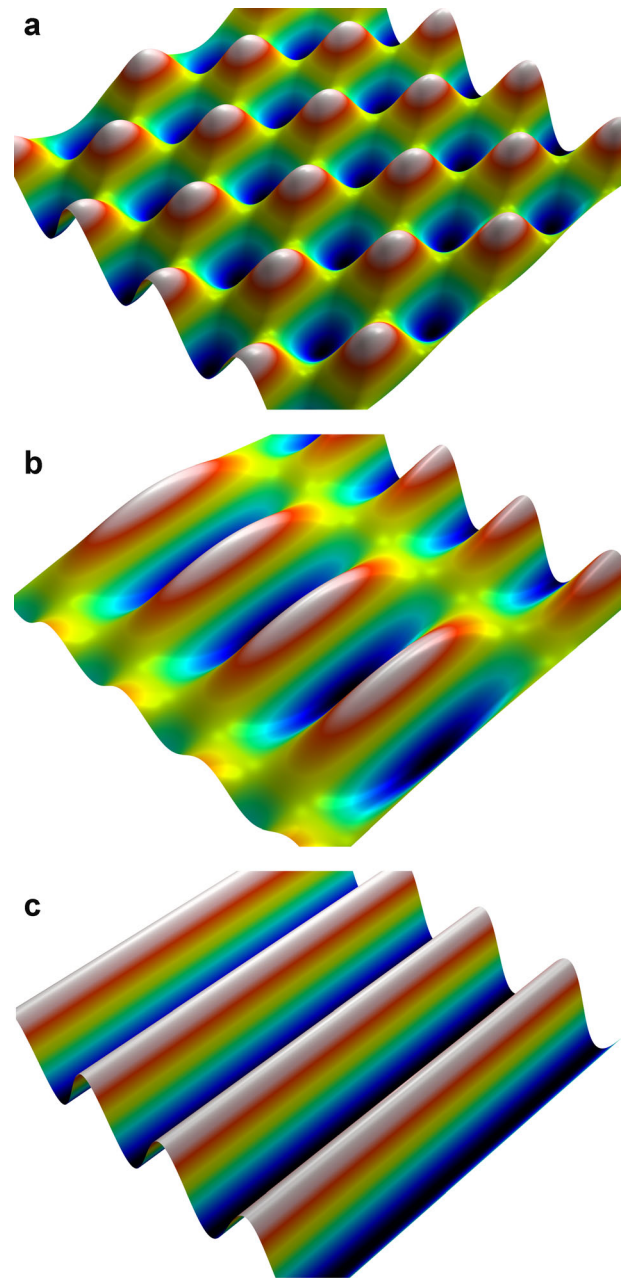
the form of a circle of radius approximately equal to 0.22%. This proves that the Gaussian noise surfaces do not have a specific anisotropic direction, which means that Gaussian noise surfaces have an isotropic shape. The regularity values are close to zero, which indicates that a pure noisy surface possesses a null regularity.

Figure 6 illustrates the anisotropy direction curves for the set of surfaces shaped according to polar coordinates. It is evident that these surfaces do not have a precise isotropy and that, therefore, the surface has no distinct periodicity direction. However, the regularity value lies between 15% and 16%, regardless of the
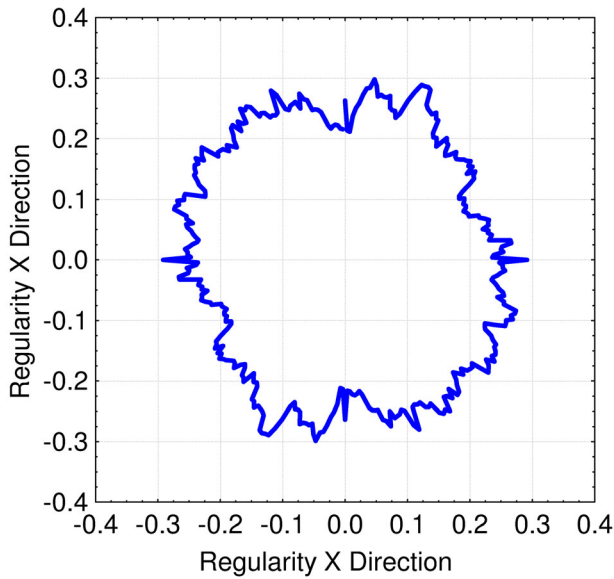
regularity parameter, which has a 90% value in these two directions. In addition, several features are noticed:

- These curves are symmetrical with respect to the 45° axis because the 2D signal is symmetrical to this axis.
- A high value of regularity is obtained at 45°. On this axis, the 2D signal is perfectly periodic, and the regularity of the surface increases.
- The order diminishes as noise decreases, keeping the shape of the curves in all directions. The method is then robust, and the regularity of the surface diminishes.
- The isotropic sine shape surface tends to a white-noise shaped surface at a very high noise level.

Figure 8 gives the anisotropy direction curves for the set of sine shape surfaces generated with a different anisotropy factor. These figures show that the higher regularity parameter is always obtained in the X_r direction, i.e. the axis along which a sinusoid is obtained, regardless of the anisotropy factor and the noise level. However, it is noticed that the regularity parameter value decreases when the anisotropy factor increases until it reaches a value of $\alpha = 6$. This is due to the fact that the more the anisotropy factor increases, the greater the difference between the generated surface and the isotropic sinusoid shape surface. However, pass over this value of $\alpha = 6$, the regularity increases in all directions (except on the X_r) to progressively obtain a perfect circle with regularity equals to the regularity in the X_r direction, i.e. 90%. In fact, curves converge to a 2D sinusoidal surface. For theses surfaces, the regularity is maximal because, whatever the direction, a period will clearly appear in the autocorrelation function **ACF** (X, Y).

The evolution of the mean regularity parameter of sine shape surfaces towards different noise levels and anisotropy factor values is represented in Figure 9. Its maximum value is about 90%. This high value identifies the periodicity of these surfaces. By adding the white Gaussian noise, this maximum value remains stable until a certain critical level of anisotropy. From this critical level, it decreases rapidly and tends to a value of 0.1. The value of the critical noise level at which the regularity parameter begins to decrease depends on the incorporated anisotropy factor. The means parameter confirms all results achieved from anisotropy direction curves, which indicates that this scalar parameter is a relevant one.

It is relevant to compare our approaches to **S**pectroscopic **A**nisotropy **M**icro-**E**llipsometry (SAME). This optical technique, also call the **R**eflection **A**nisotropy **S**pectroscopy (RAS), allows quantification of the regularity of a surface at a nanoscopic level, i.e. the molecular assembly of ordered surfaces (Aspnes *et al.*, '88). The reflected light yields information on anisotropy of the surface, due to the interaction of

Fig 5. Anisotropy direction curves for the set of white noise surfaces.

direction. This means that the surfaces are quite isotropic. It can be noticed that the level of order is quite low, as determined by the fact that the curves create a perfect periodic shape in polar coordinates, if and only if the origin is taken at zero: the periodicity is only constant for this case. If a profile is extracted randomly from the surface, the period will never be stationary, as can be seen on the ACF in Figure 2b; as a consequence, the order never reaches 100%.

Figure 7 represents the anisotropy direction curves that belong to the set of isotropic sine surfaces. In these surfaces, the perfect sine form is clearly identified in the X and Y directions. It is detected in Figure 7 by the
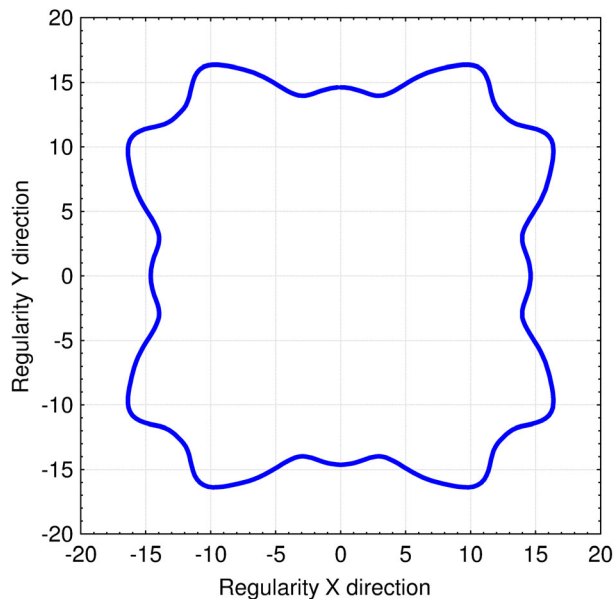

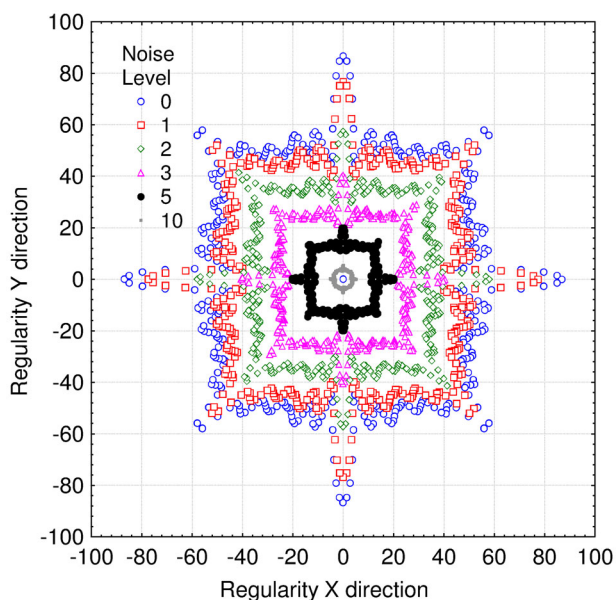**Fig 6.** Anisotropy direction curves for the set of polar surfaces.

Fig 7.   Anisotropy direction curves for the set of isotropic sine surfaces with different noise levels.

radiation with matter and the use of Jones vector/matrices as models (Berkovits *et al.*, '85). Using a linear optical probe with visible light, this nondestructive method (Weightman *et al.*, 2005) is well adapted to quantify the self-assembly of nanostructures, i.e. Epioptic techniques (McGilp, '95; Richter and McGilp, '93). This method permits a quantifying of the perfect symmetry of a crystallographic plane: the (100) on a FCC is perceived as perfectly structured (no roughness), and FCC(110) surfaces possess intrinsic structural anisotropy. The state of a surface on clean Cu can be described as a 2D, nearly free electron gas. The
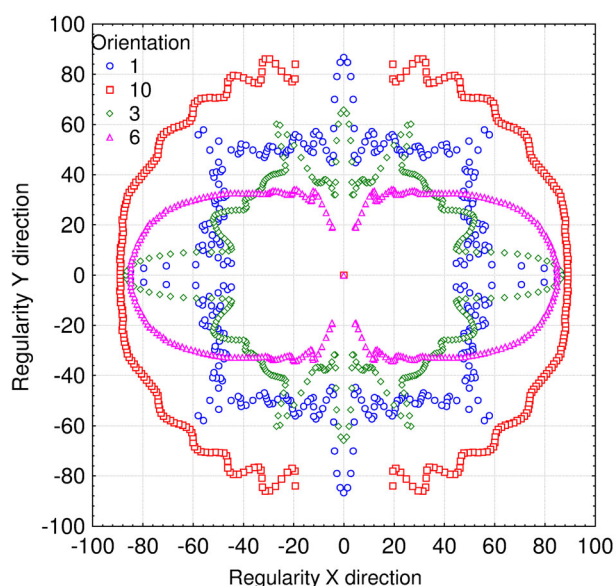
RAS allows quantifying order the occupied surface state on Cu(111), after the surface is confined by a circle of Fe atoms (Sun *et al.*, 2003). RAS can be used to monitor molecular assembly on macroscopic ordered surfaces, where the surface induces order in the molecular layer substrate-influenced molecular assembly to create a chemically functionalized surface. Using the Monte-Carlo simulation, Bigerelle *et al.* have shown that the order of these surfaces increases during the self-assembly processes (Bigerelle *et al.*, 2006). In a purely topographical process, Martin *et al.* prepared flat and smooth metal surfaces for molecular adsorption in an aqueous environment (Isted and Martin, 2005) and showed that peaks on the RAS spectrum result from the modification of the anisotropy of the surface (Martin *et al.*, 2004). The aim of using RAS to quantify the order of the roughness is particularly illustrated on the change of the S_q (RMS) of the Au(110) ion bombardment surface, which decreases the regularity of the surface (Martin *et al.*, 2003).

The regularity parameter can be used in multiple applications:

- To identify the direction of periodical structures formed by laser pulsed radiations (Young et al., '83; Pedraza et al., 2003; Zheng *et al.*, 2009) on the surface of solid workpieces. This identification qualifies the success of the process, since the structures appear only in a certain range of pulse duration and power, depending on a radiation wavelength and on the material's surface conditions (Syvenkyy *et al.*, 2007).
- To examine the reproducibility of surface machining methods such as the finishing process (Barletta, 2006), by comparing the values of this parameter on several specimens on which the same process conditions have been applied.
- To identify the surface regularity produced by abrasive machining, such as precision surface grain,

Fig 8.   Anisotropy direction curves for the set of anisotropic sine surfaces.
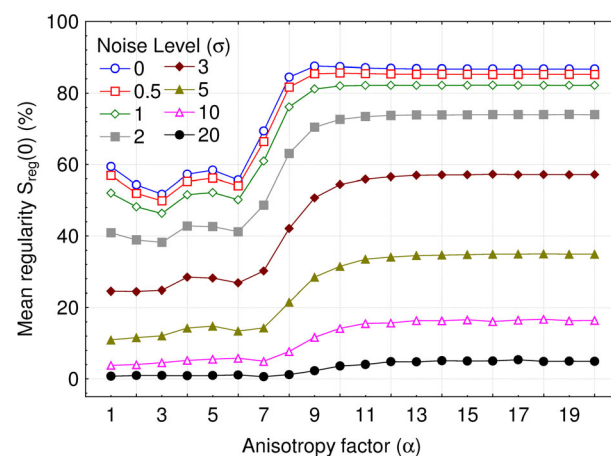

Fig 9.   Evolution of the mean regularity parameter ($\lambda = 0$) versus the noise level for the generated sine surfaces associated to different anisotropy factor (α).

abrasive slotting, and lapping (Ohbuchi and Matsuo, '95; Chardrasekar et al., '87).

Conclusion

A nondimensional parameter is defined and tested, in order to characterize the regularity of surface topography. It was shown that the isotropy of surface roughness was identified using this parameter. The regularity parameter can thus be termed an "isotropy index" and can be used to quantify the influence of different processes on surface topography. This parameter quantifies the effect of noise in the surface. On a perfect, uncorrelated surface, a value close to zero of this parameter was found. The anisotropy direction is well identified by the regularity parameter. This essential information could be used to measure the most typical roughness surface. This unscaled parameter is complementary to the autocorrelation length to assess the long range structure of the surface autocorrelation. For noisy isotropic surfaces, the order parameter is around 0.3%, and 80% for a perfect 2D sinusoid surface.

This parameter can be used in a multi-scale analysis to quantify the scale on which order will appear, by maximizing its value during multi-scale decomposition. Despite the good results obtained in this application, further experimental works remain to be done, in order to validate the formula of the regularity parameter.

References

Aspnes DE, Harbison JP, Studna AA, Florez LT. 1988. Reflectance-difference spectroscopy system for real-time measurements of crystal growth. Appl Phys Lett 52:957–959.

Barletta M. 2006. A new technology in surface finishing: fluidized bed machining (FBM) of aluminium alloys. J Mater Proc Tech 173:157–165.

Benardos PG, Vasniakos GC. 2003. Predicting surface roughness in machining: a review. Int J Mach Tools Manuf 43:833–844.

Berkovits VL, Makarenko IV, Minashvili TA, Safarovl VI. 1985. Optical transitions on GaAs [110] surface. Solid State Commun 56:49–450.

Bigerelle M, Haidara A, Van Gorp A. 2006. Monte Carlo simulation of gold nano-colloids aggregation morphologies on a heterogeneous surface. Mater Sci Eng C 26:1111–1116.

Bhushan B. 1999. Principles and applications of tribology. New York: Wiley.

Chardrasekar S, Shaw MC, Bhushan B. 1987. Morphology of ground and lapped surfaces of ferrite and metals. Trans ASME J Eng Ind 109:83–86.

Chien JH, Shiau D, Halford JJ, et al. 2011. A signal regularity-based automated seizure prediction algorithm using long-term scalp EEG recordings. Cybern Syst Anal 47:586–597.

DIN4760. 1982. Form Deviations, Concepts, Classification System. Deutches Institut Fuer Normung.

Dong WP, Stout KJ. 1995. Two-dimensional fast Fourier transform and power spectrum for surface roughness in three dimensions. Proc Inst Mech Eng Part B J Eng Manuf 209:381–391.

Dubuc B, Zucker SW, Tricot C, Quiniou JF, Wehbi D. 1989. Evaluating the fractal dimension of surfaces. Proc R Soc Lond Ser A Math Phys Sci 425:113–127.

Isted GE, Martin DS. 2005. Preparation and characterisation of Au (1 1 0) and Cu(1 1 0) surfaces for applications in ambient environments. Appl Surf Sci 252:1883–1890.

McGilp J. 1995. Optical characterisation of semiconductor surfaces and interfaces. Prog Surf Sci 49:1–106.

Mallat S. 1989. A theory for multiresolution signal decomposition: the wavelet representation. IEEE Trans Pattern Anal Mach Intell 11:674–693.

Martin DS, Cole RJ, Blanchard NP, et al. 2004. Contributions from surface-modified bulk electronic bands to the reflection anisotropy of Au (110)-(1 × 2). Condens Matter 16:S4375–S4379.

Martin DS, Blanchard NP, Weightman P. 2003. The effect of surface morphology upon the optical response of Au (110). Surf Sci 532–535:1–7.

Novák D, Kremen V, Cuesta D, et al. 2009. Discrimination of endocardial electrogram disorganization using a signal regularity analysis. Conf Proc IEEE Eng Med Biol Soc 1:1812–1815.

Ohbuchi Y, Matsuo T. 1995. Chipping in high-precising solt grinding of Mn–Zn ferrite. CIRP Ann 44:273–277.

Pedraza AJ, Fowlkes JD, Guan YF. 2003. Surface nanostructuring of silicon. Appl Phys A 77:277–284.

Richter W, McGilp J. 1993. Optical in situ surface control during MOVPE and MBE growth. Phil Trans R Soc Lond 344:444–467.

Sun LD, Hohage M, Zeppenfeld P, Balderas-Navarro RE, Hinger K. 2003. Surface-induced d-band anisotropy on Cu(110). Surf Sci Lett 527:184–190.

Syvenkyy Y, Kotlyarchuk B, Savchuk V, et al. 2007. Laser-induced formation of periodical structures on the A^{II}B^{VI} semiconductors surfaces. Opt Mater 30:380–383.

Venkateh K, Bobji MS, Gargi SK. 1999a. Genesis of workpiece roughness generated in surface grinding and polishing of metals. Wear 225:226–251.

Venkateh K, Bobji MS, Gargi SK. 1999b. Power spectra of roughness caused by grinding of metals. J Mater Res 14:319–322.

Weiting C, Wangxin G, Guitao C. 2009. A new method assessing signal regularity. Sixth Int Conf Fuzzy Syst Knowl Discov 5:563–566.

Weightman P, Martin DS, Cole RJ, Farrell T. 2005. Reflection anisotropy spectroscopy. Rep Prog Phys 68:1251–1289.

Whitehouse DJ. 2011. Handbook of surface and nanometrology. New York: CRC Press, Taylor & Francis.

Young JF, Sipe JE, Van Driel HM. 1983. Regimes of laser-induced periodic surface structure on germanium: radiation remnants and surface plasmons. Opt Lett 8:431–433.

Zheng HY, Tan TT, Zhow W. 2009. Studies of KrF laser-induced long periodic structures on polyimide. Opt Lasers Eng 47:180–185.